

Electronic Supplementary Information

Near-Infrared Fluorescent Turn-On Probe for Hydrazine Detection: Environmental Samples and live cell imaging

Anwasha Maiti,^a Dipanjan Banik,^a Satyajit Halder,^b Saikat Kumar Manna,^c Anirban Karak,^a Kuladip Jana,^b and Ajit Kumar Mahapatra^{a*}

^aMolecular Sensor and Supramolecular Chemistry Laboratory, Department of Chemistry, Indian Institute of Engineering Science and Technology, Shibpur, Howrah-711103, West Bengal, India, E-mail: akmahapatra@chem.iiests.ac.in

^bDivision of Molecular Medicine, Bose Institute, P 1/12, CIT Scheme VIIM, Kolkata-700054, India.

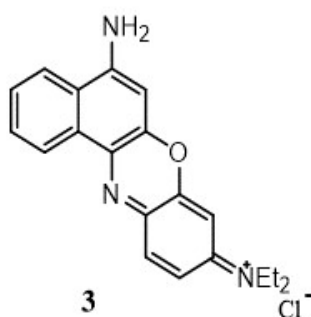
^c Department of Chemistry, Haldia Government College, Debhog, Haldia, Purba Medinipur-721657, West Bengal, India.

Table of Contents

1. NMR Characterization data of compound **3** and **4**.
2. ¹H NMR of compound **3** in MeOH-d₄.
3. ¹³C NMR of compound **3** in MeOH-d₄.
4. ¹H NMR of compound **4** in DMSO-d₆.
5. ¹³C NMR of compound **4** in DMSO-d₆.
6. HRMS of probe **BPN**.
7. ¹H NMR of probe **BPN** in DMSO-d₆.
8. ¹³C NMR of probe **BPN** in DMSO-d₆.
9. UV-vis absorbance spectra, fluorescence emission spectra and quantum yield of compound **3**
10. UV-vis absorbance spectra, fluorescence emission spectra and quantum yield of compound **4**.
11. UV-vis absorbance of probe **BPN**.
12. Comparative Fluorescence spectrum of compound **4** and **R1**.
13. Comparative UV-vis absorption spectrum of probe **BPN**, Compound **3** and **BPN** treated with N₂H₄.
14. Comparative Fluorescence spectrum of probe **BPN**, Compound **3** and **BPN** treated with N₂H₄.
15. Change of fluorescence emission intensity of **BPN** upon addition of interfering analytes and then hydrazine.
16. Change of fluorescence emission intensities of **BPN** in presence of hydrazine and other interfering analytes in 1:1 and n:1 crowded environments.
17. Detection limit calculation.
18. Kinetic plot of probe **BPN**.

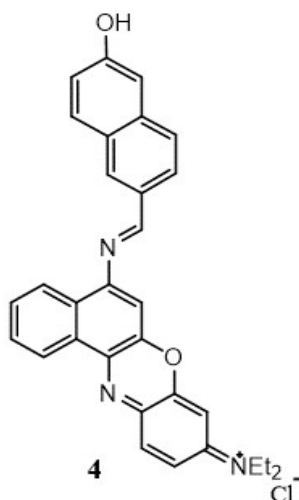
19. Fluorescence quantum yield calculation.
20. MTT assay for determination cytotoxic effect of probe **BPN** on MDA-MB 231 cells.
21. Pictorial fluorescence intensity change of untreated cell and cell treated with hydrazine.
22. HRMS of **BPN-N₂H₄ adduct**.
23. ¹H NMR titration of probe **BPN** upon addition of hydrazine.
24. Summary of previously reported hydrazine sensing fluorescent chemosensors with latest work.
25. References.

Structure and NMR characterization data of compounds 3,4:



¹H NMR (400 MHz, MeOH-d₄): δ 0.63 (t, J=8.0Hz, 6H), 1.25(q, J=8.0Hz, 4H), 3.71 (s, 2H), 4.75 (s, 1H), 5.33 (d, J=8.0Hz, 2H), 6.43 (s, 1H), 7.30 (t, J=8.0Hz, 2H), 7.87 (d, J=8.0Hz, 1H), 7.96 (d, J=8.0Hz, 1H).

¹³C NMR (400 MHz, MeOH-d₄): δ 11.40 (2C), 44.20 (2C), 90.50 (1C), 111.79 (1C), 120.21 (1C), 120.50 (1C), 121.20 (1C), 122.21 (1C), 122.70 (1C), 123.69 (1C), 123.96 (1C), 124.07 (2C), 125.30 (1C), 132.06 (1C), 140.07 (1C), 145.96 (1C), 148.77 (1C).



¹H NMR (400 MHz, DMSO-d₆): δ 1.26 (t, J=8.0Hz, 6H), 3.08 (s, 1H), 3.46 (q, J=8.0Hz, 4H), 5.39 (d, J=8.0Hz, 2H), 6.19 (s, 1H), 7.01 (d, J=8.0Hz, 2H), 7.03 (s, 1H), 7.05 (d, J=8.0Hz, 2H), 7.54 (t, J=8.0Hz, 2H), 7.96 (d, J=8.0Hz, 2H), 7.99 (d, J=8.0Hz, 1H), 9.50 (s, 1H), 11.0 (s, 1H).

¹³C NMR (400 MHz, DMSO-d₆): δ 11.43 (2C), 44.70 (2C), 90.82 (1C), 99.38 (1C), 112.40 (1C), 120.21 (1C), 120.55 (1C), 121.24 (6C), 122.60 (1C), 122.77 (2C), 123.69 (2C), 123.71 (1C), 123.74 (2C), 126.06 (2C), 130.70 (1C), 132.45 (1C), 142.52 (1C), 149.31 (1C), 160.82(1C), 162.08 (1C).

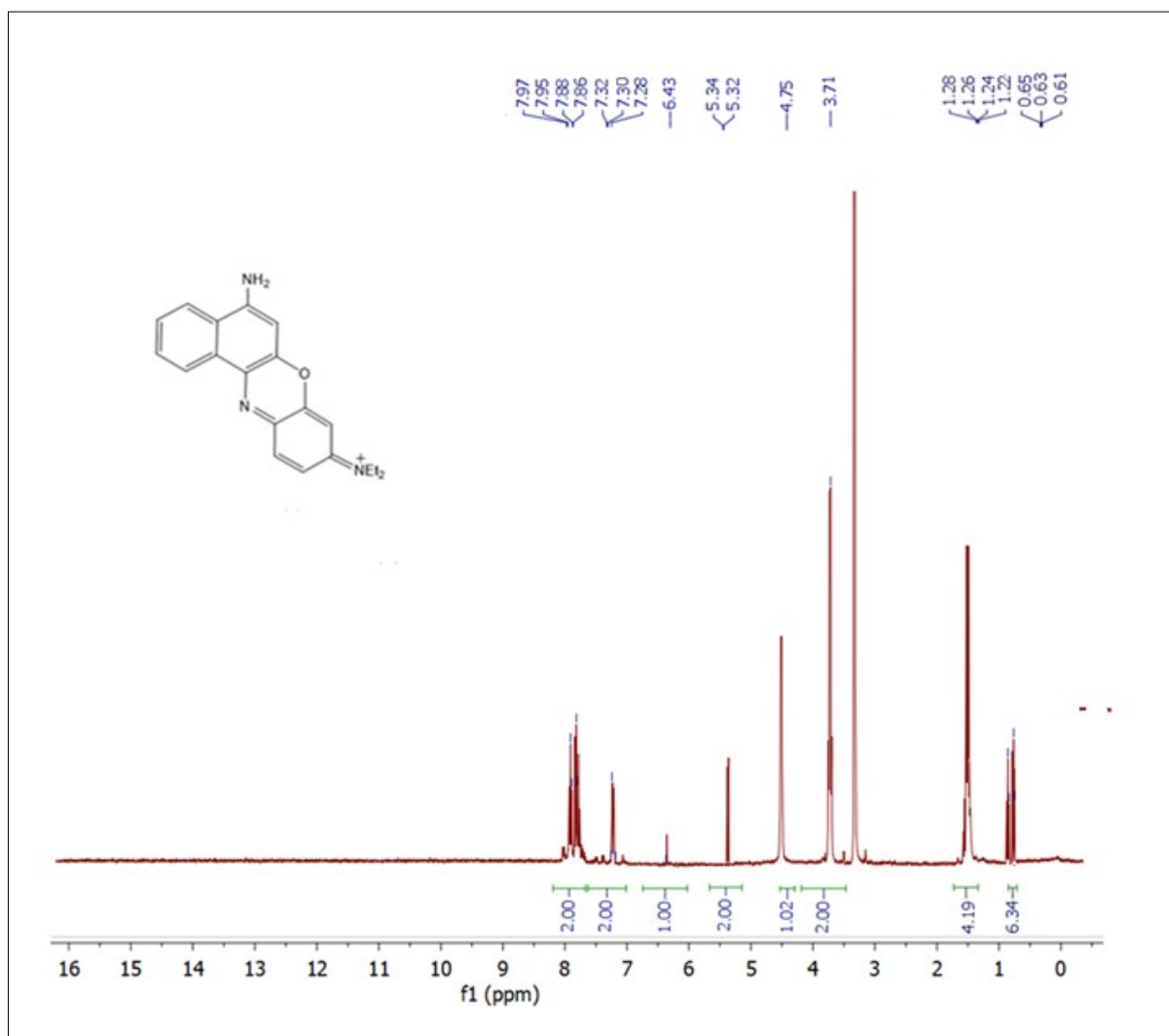


Figure S1: ¹H NMR of compound 3 in MeOH-d₄

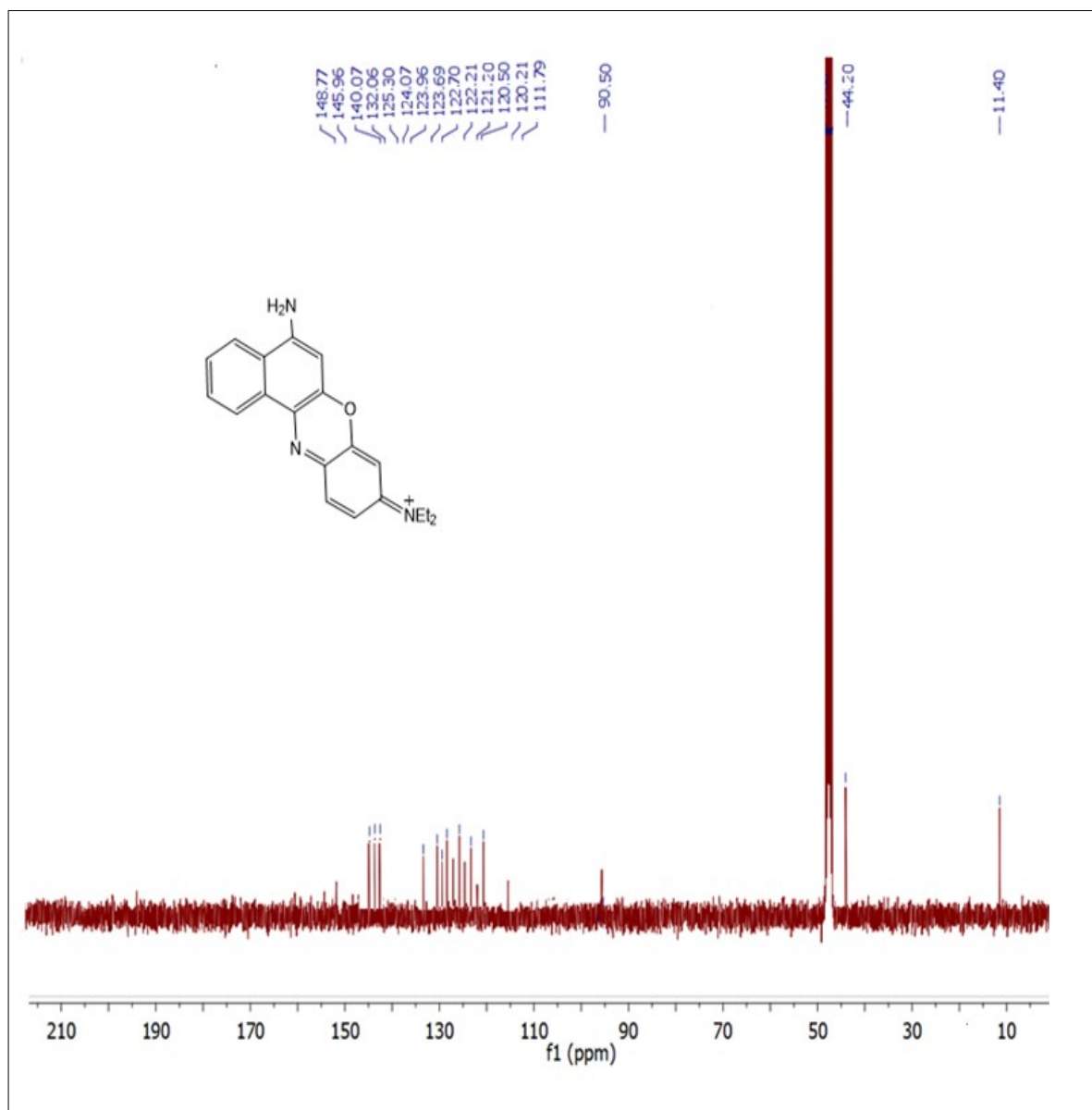


Figure S2: ^{13}C NMR of compound **3** in MeOH-d_4

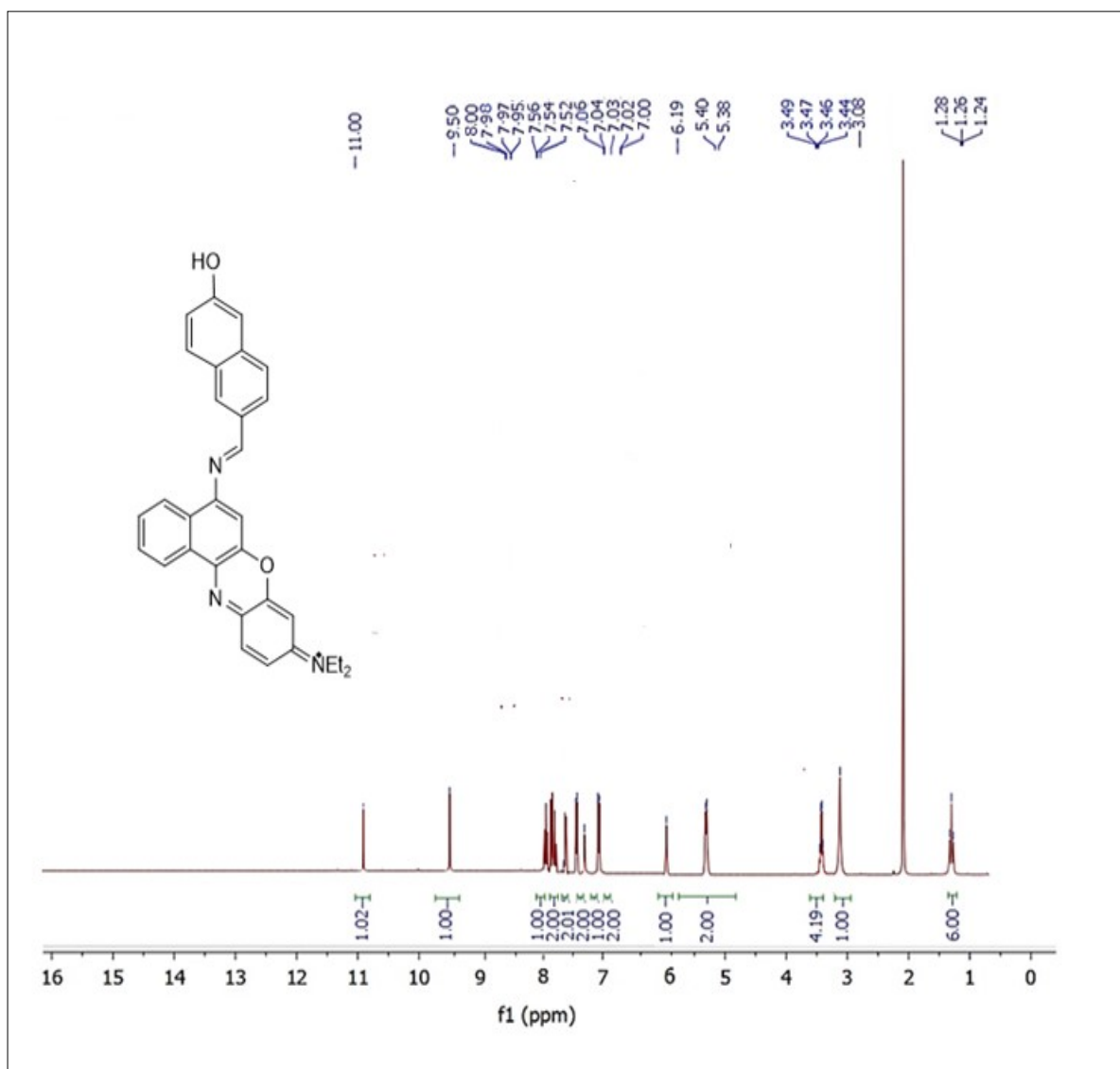


Figure S3: ¹H NMR of compound 4 in DMSO-d₆

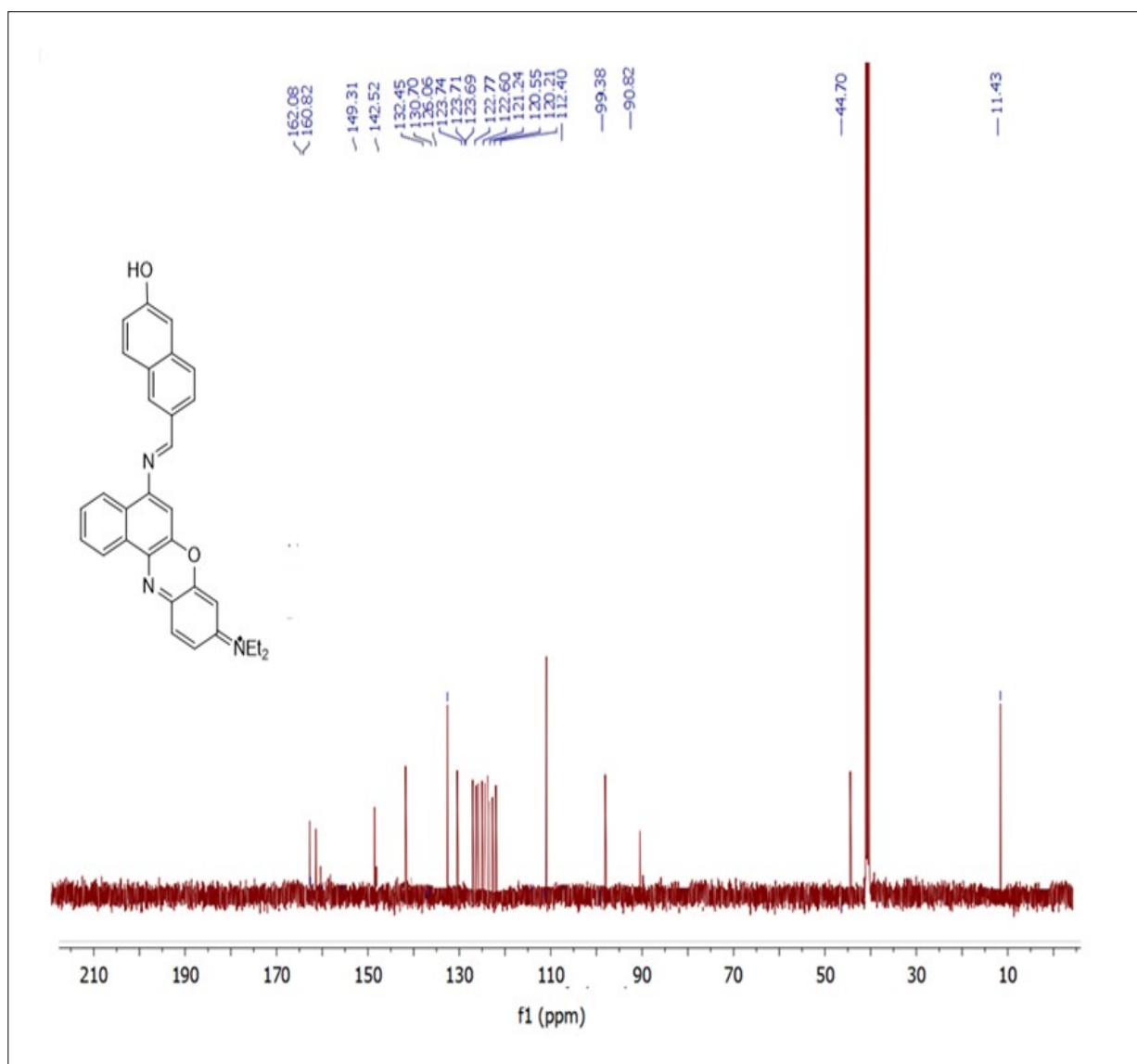


Figure S4: ¹³CNMR of compound 4 in DMSO-d₆

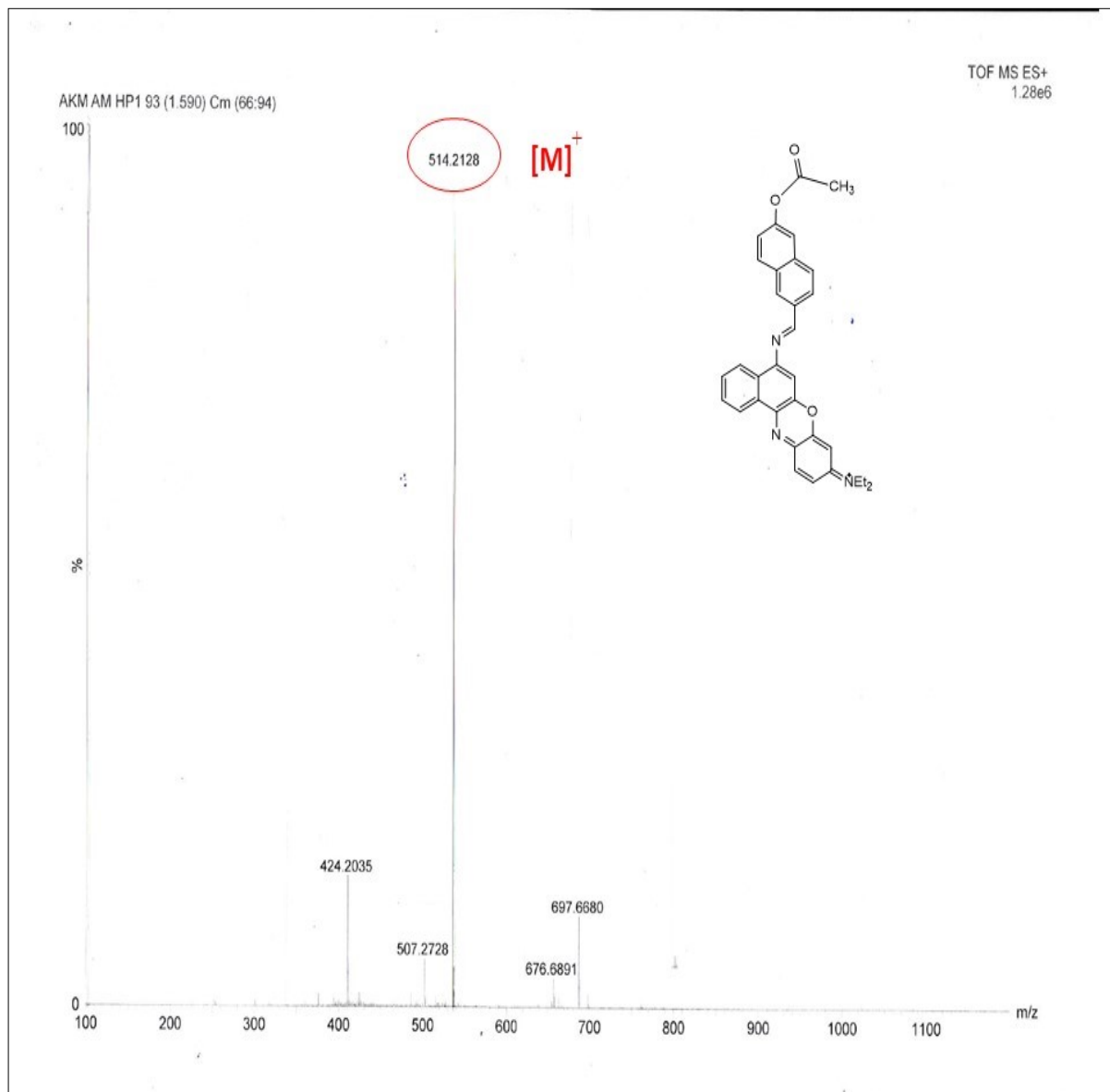


Figure S5: HRMS of probe **BPN**

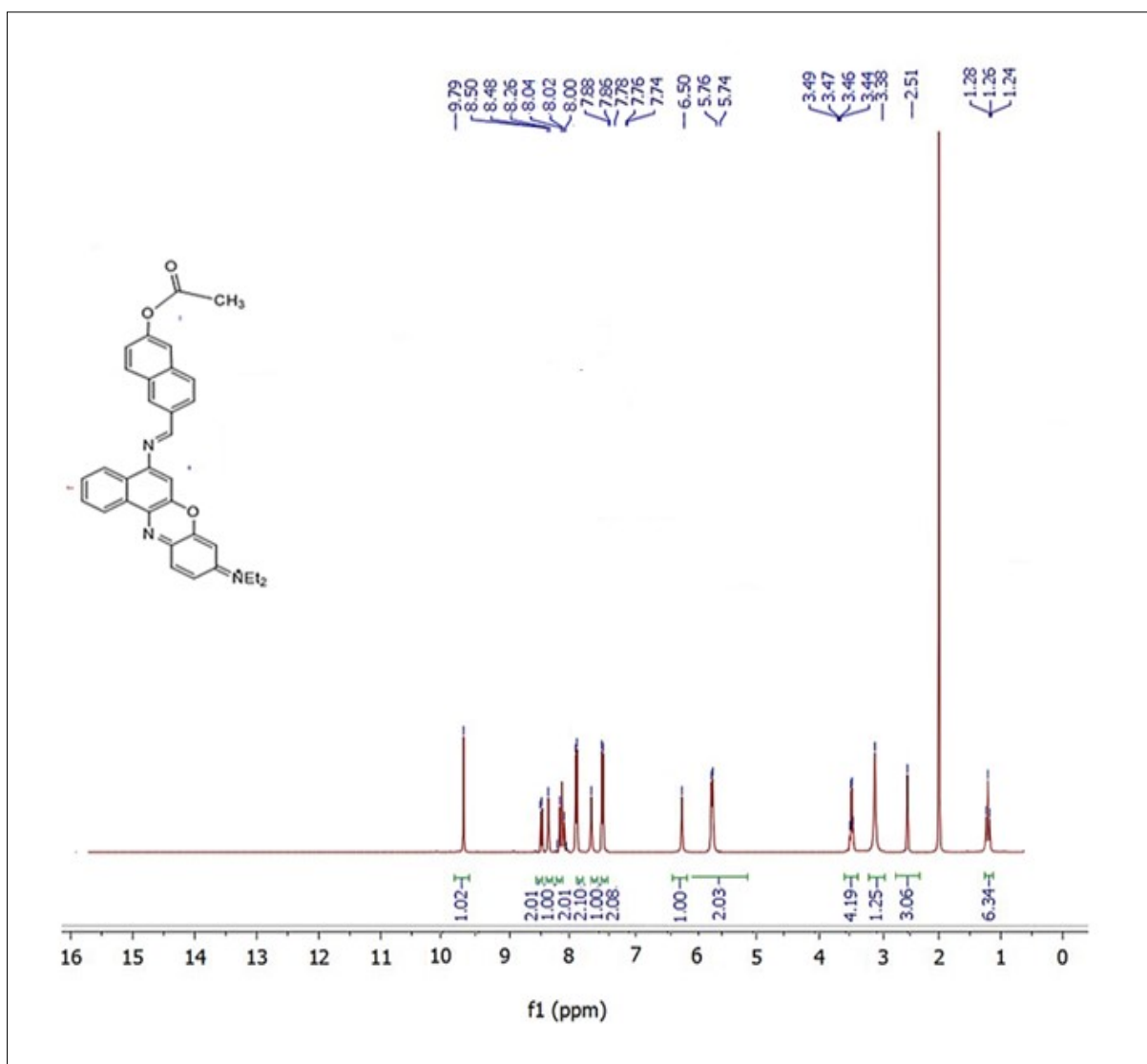


Figure S6: ¹H NMR of probe BPN in DMSO-d₆

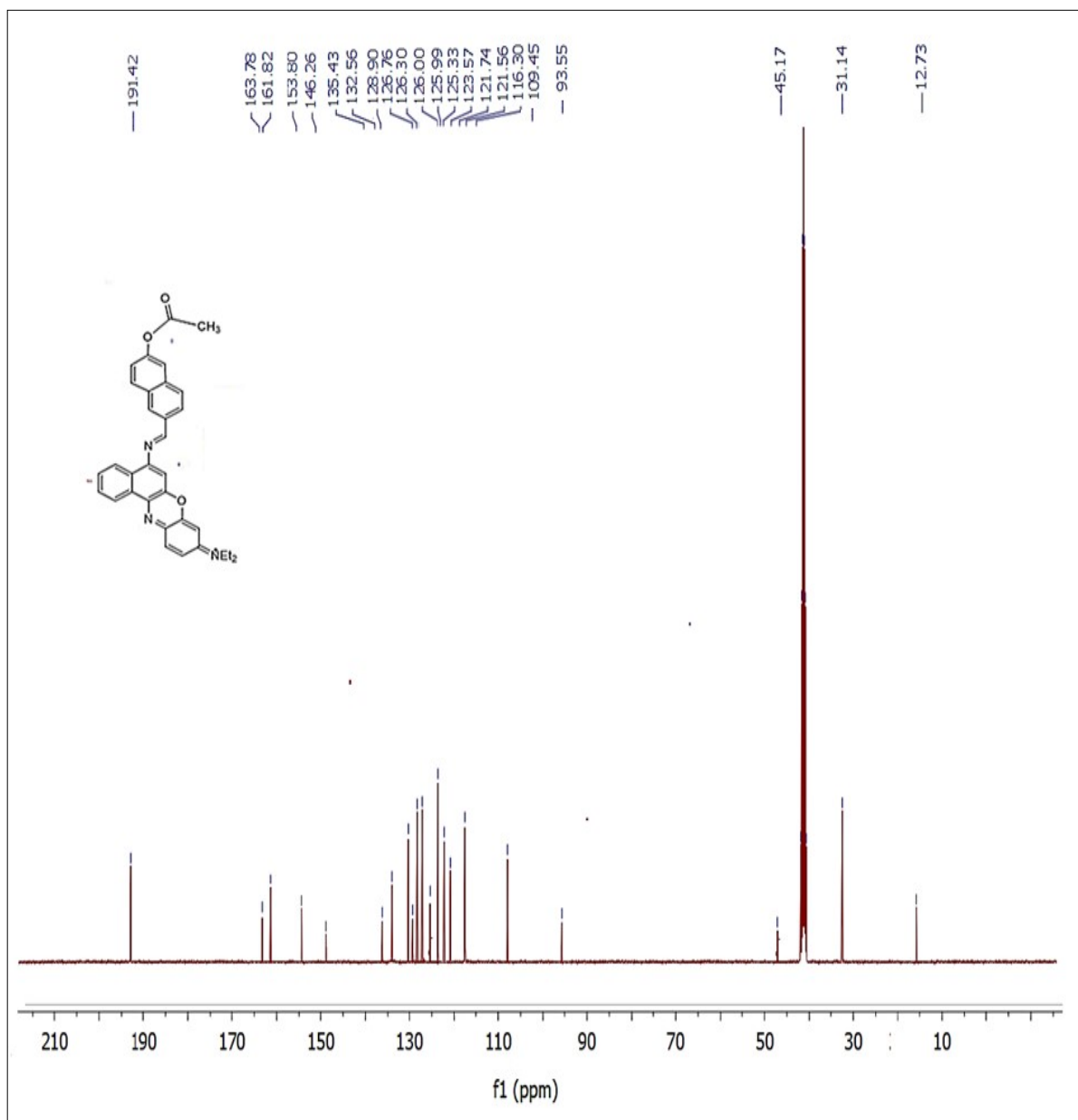
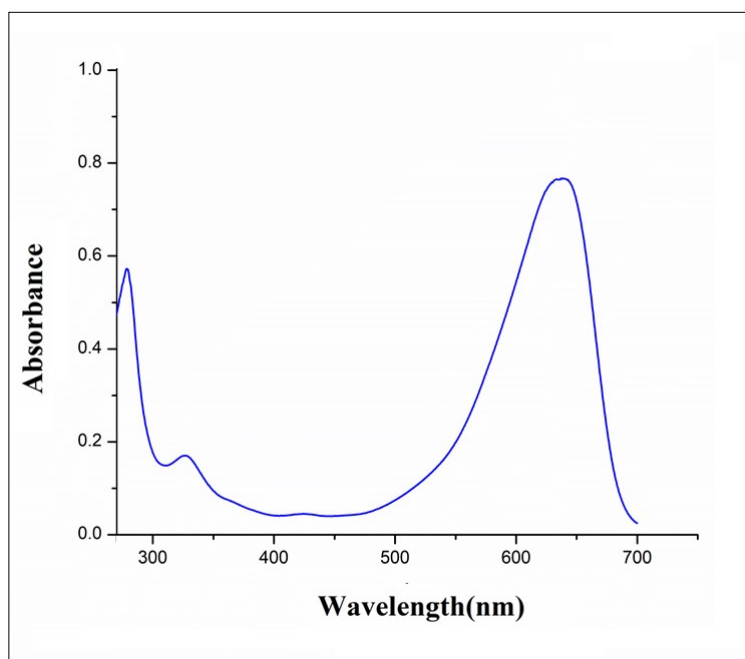


Figure S7: ^{13}C NMR of probe BPN in DMSO-d_6



FigureS8:UV-vis absorbance of compound 3 ($c = 4 \times 10^{-5}$ M) in aq. DMSO (DMSO/H₂O = 1:9 v/v, 10 mM PBS buffer, pH = 7.4).

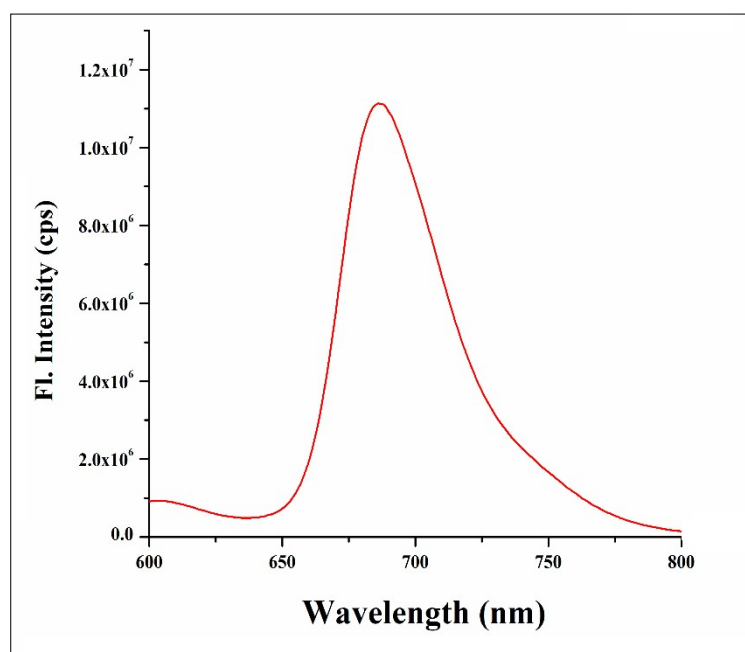


Figure S9: Fluorescence spectrum of compound 3 ($c = 4 \times 10^{-5}$ M) in aq. DMS(DMSO/H₂O = 1:9 v/v, 10 mM PBS buffer, pH = 7.4).

The quantum yield of compound 3 is 0.28 using Rhodamine B in ethanol as standard.

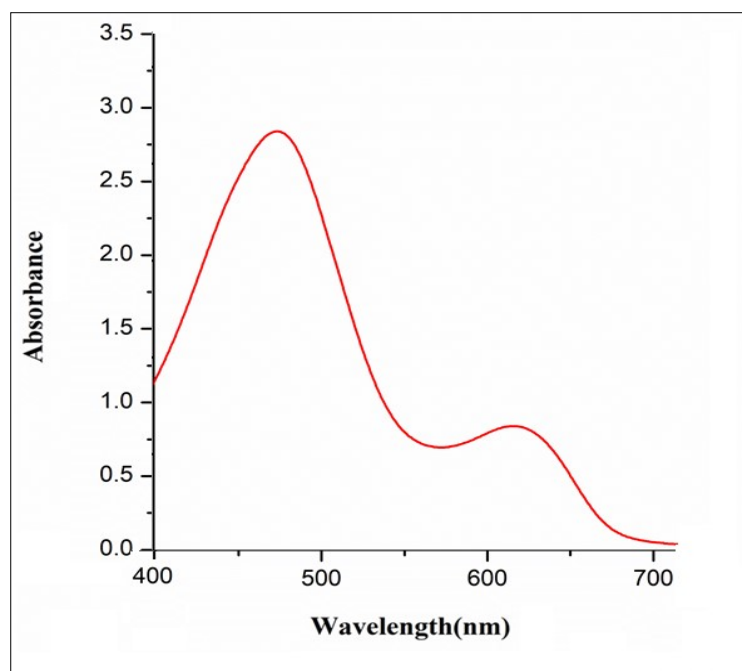


Figure S10: UV-vis absorbance of compound 4 ($c = 4 \times 10^{-5}$ M) in aq. DMSO (DMSO/H₂O = 1:9 v/v, 10 mM PBS buffer, pH = 7.4).

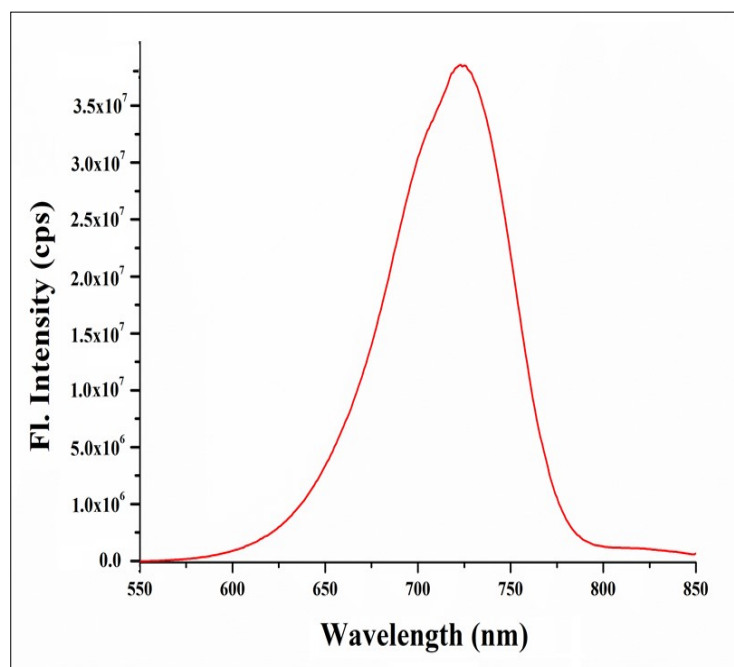


Figure S11: Fluorescence spectrum of compound 4 ($c = 4 \times 10^{-5}$ M) in aq. DMSO (DMSO/H₂O = 1:9 v/v, 10 mM PBS buffer, pH = 7.4).

The quantum yield of compound 4 is 0.62 using Rhodamine B in ethanol as standard.

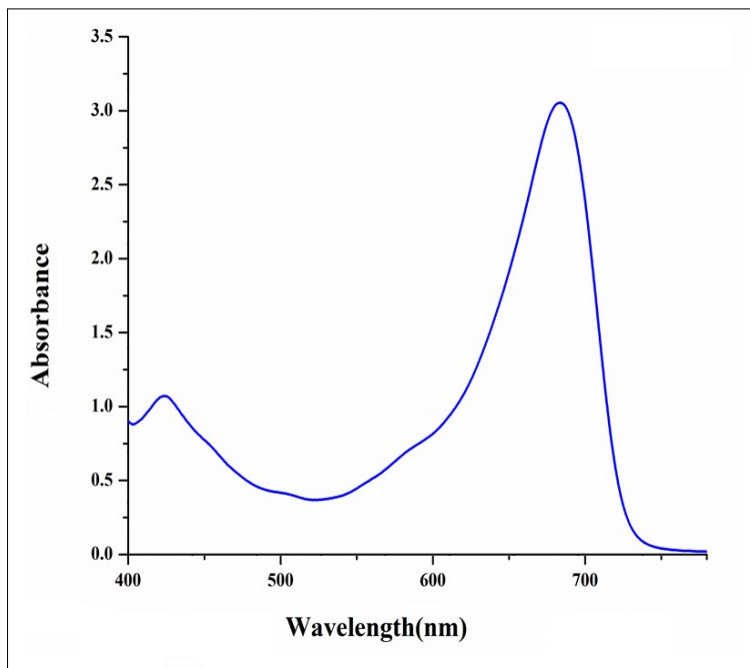


Figure S12: UV-vis absorbance of probe BPN ($c = 4 \times 10^{-5}$ M) in aq. DMSO (DMSO/H₂O = 1:9 v/v, 10 mM PBS buffer, pH = 7.4).

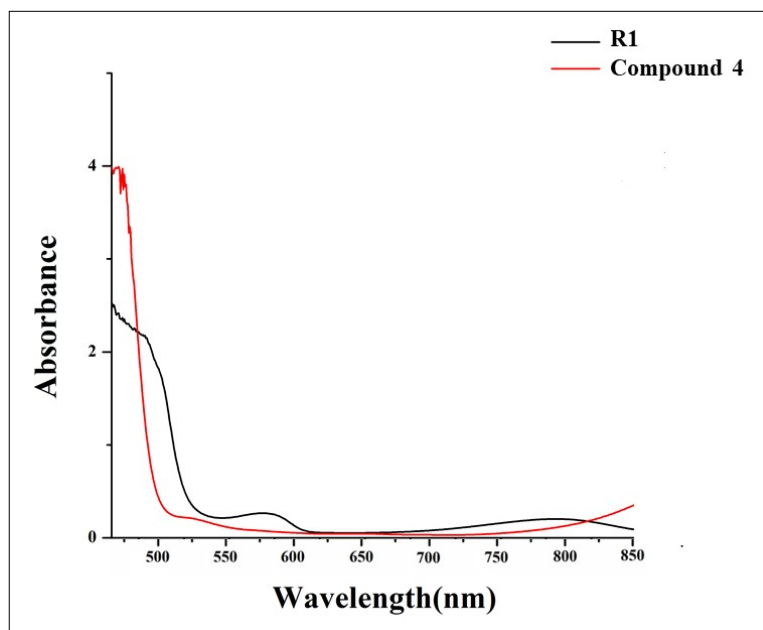


Figure S13: Comparative UV-vis absorption spectrum of compound 4 and R1 ($c = 4 \times 10^{-5}$ M) in aq. DMSO (DMSO/H₂O = 1:9 v/v, 10 mM PBS buffer, pH = 7.4)

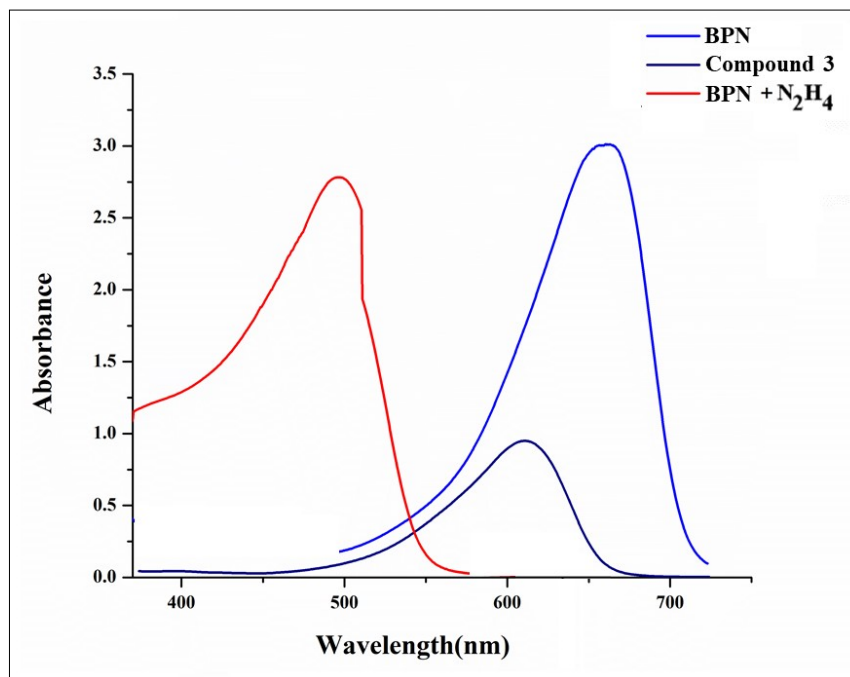


Figure S14: Comparative UV-vis absorption spectrum of probe BPN, Compound 3 and BPN treated with N₂H₄ ($c = 4 \times 10^{-5}$ M) in aq. DMSO (DMSO/H₂O = 1:9 v/v, 10 mM PBS buffer, pH = 7.4).

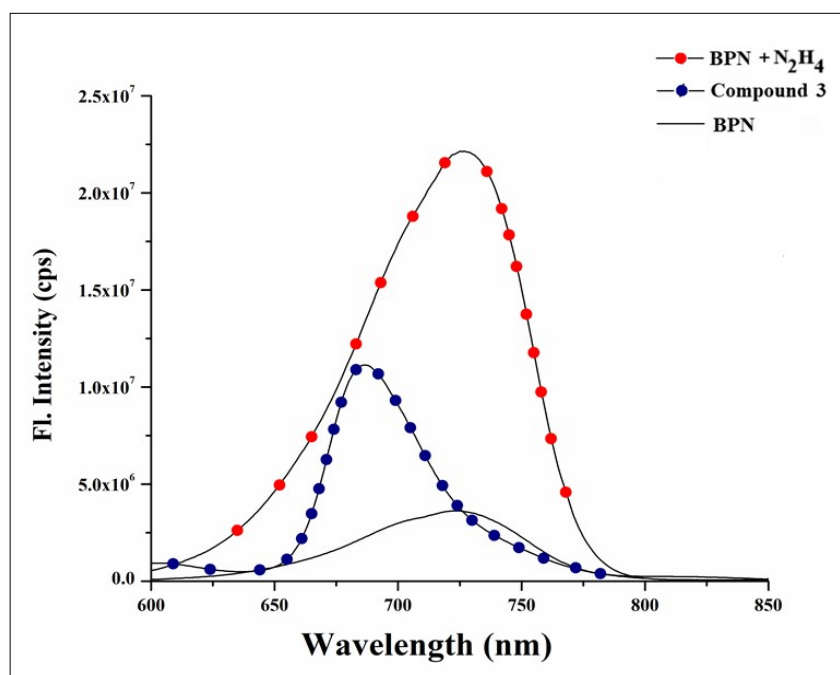


Figure S15: Comparative Fluorescence spectrum of probe BPN, Compound 3 and BPN treated with N₂H₄ ($c = 4 \times 10^{-5}$ M) in aq. DMSO (DMSO/H₂O = 1:9 v/v, 10 mM PBS buffer, pH = 7.4).

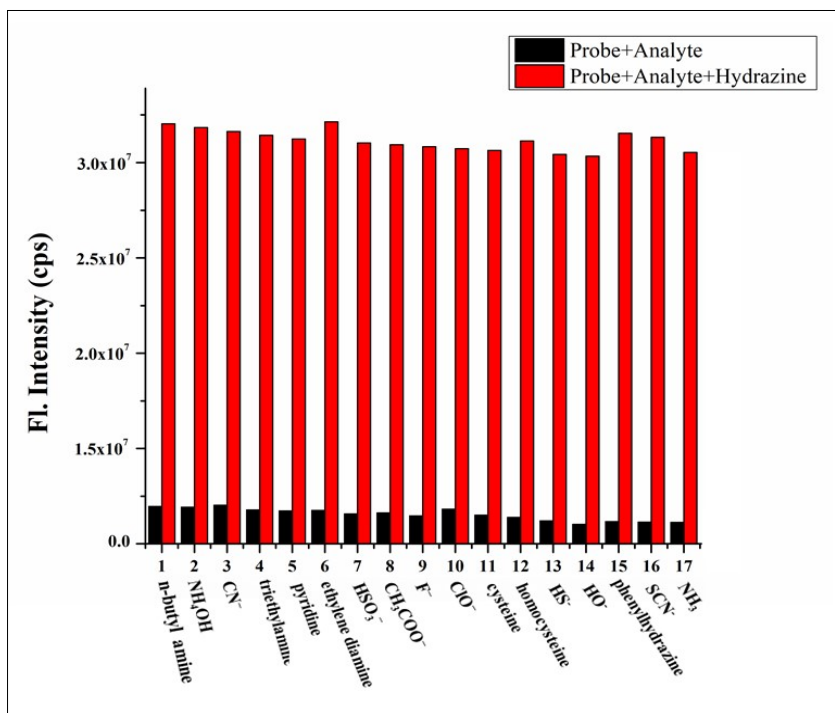


Figure S16: Change of fluorescence emission intensities of **BPN** ($c = 4 \times 10^{-5}$ M) upon addition of other interfering analytes (20 equivalents) and then hydrazine (10 equivalents).

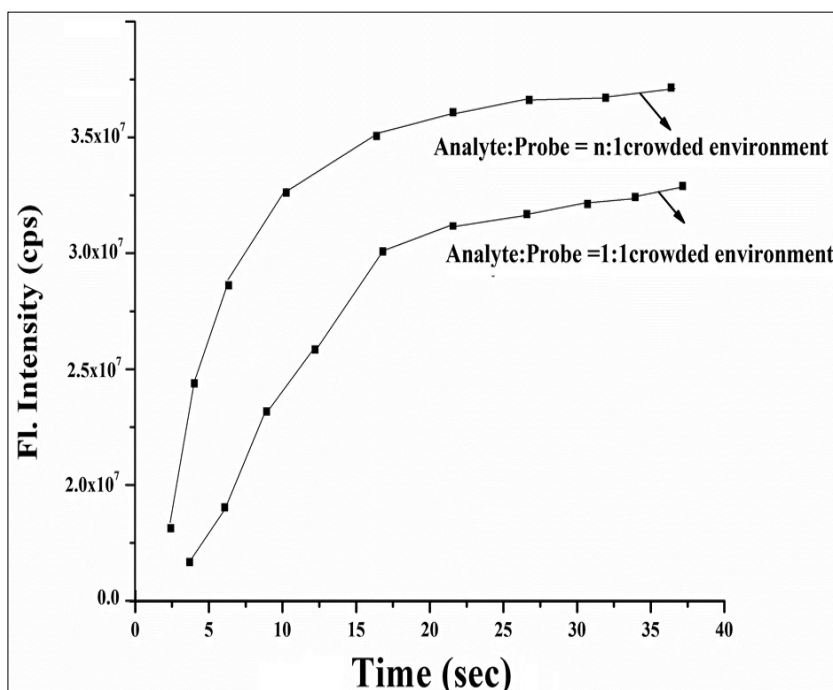


Figure S17: Change of fluorescence emission intensities of **BPN** in presence of hydrazine and other interfering analytes both in 1:1 and n:1 crowded environment.

Calculation of Detection limit:

By using the following equation $DL = K \cdot S_{b1} / S$; the detection limit (DL) of probe BPN for N_2H_4 was calculated, where $K = 2$ or 3 (we take 2 in this case); S_{b1} is the standard deviation of the blank solution; S is the slope of the calibration curve.

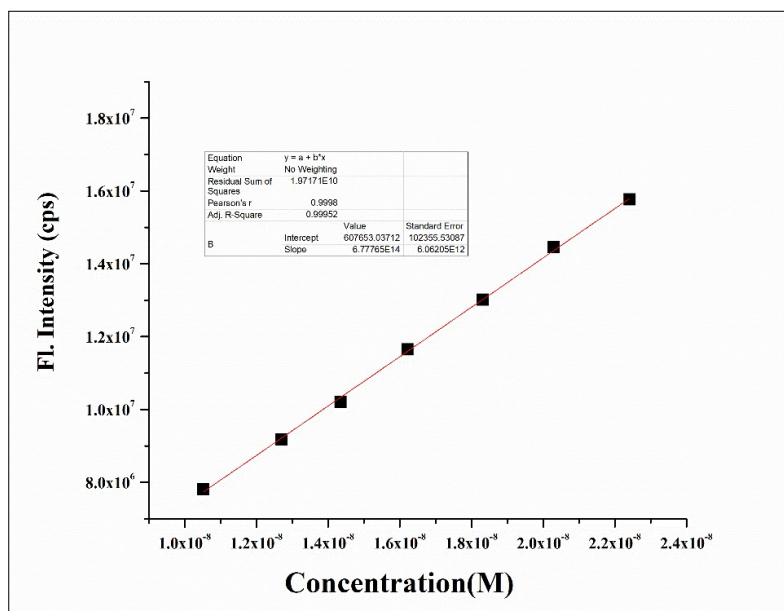


Figure S18: From the graph we get slope (S) = 6.77765×10^{14} , Standard deviation ($S_{b1} = 102355.53087$). Thus, using the formula, we get the detection limit = 4.5×10^{-10} M

Kinetic study of probe BPN:

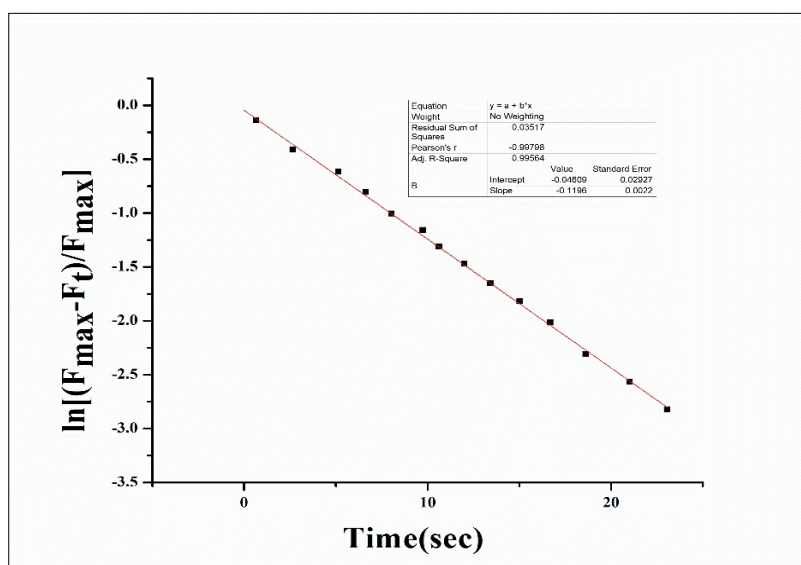


Figure S19: Pseudo first order kinetic diagram of probe BPN (1×10^{-5} M) with N_2H_4 (1×10^{-4} M) in DMSO- H_2O .

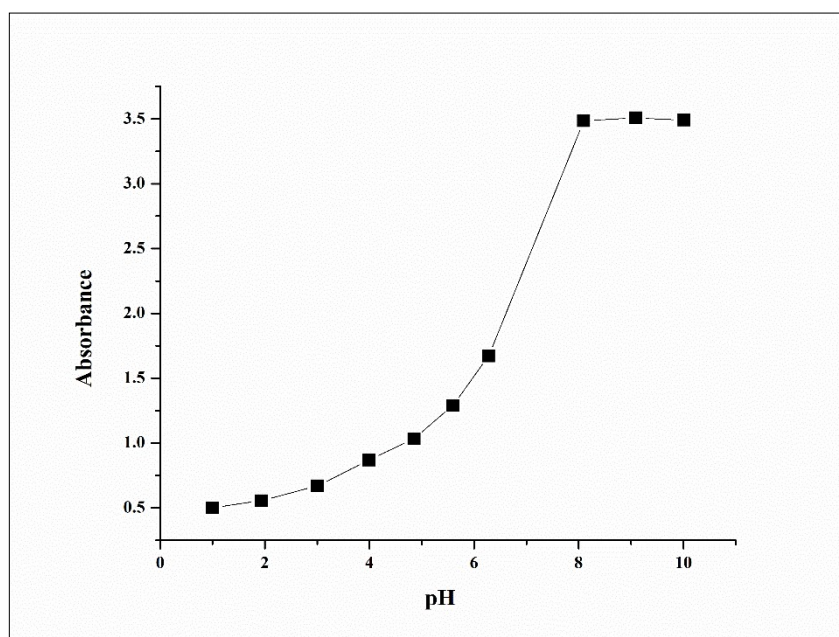


Figure S20: pH mediated absorbance change of probe **BPN** in presence of hydrazine.

Calculation of fluorescence quantum yield of **BPN** and **BPN-N₂H₄** adduct:

Here, the fluorescence quantum yield Φ was calculated by using the following equation:

$$\Phi_x = \Phi_s (F_x/F_s) (A_s /A_x) (\eta_x^2 / \eta_s^2)$$

Where,

X and S indicate the unknown and standard solution respectively, Φ = quantum yield

F = Area under the emission curve, A= Absorbance at the excitation wavelength,

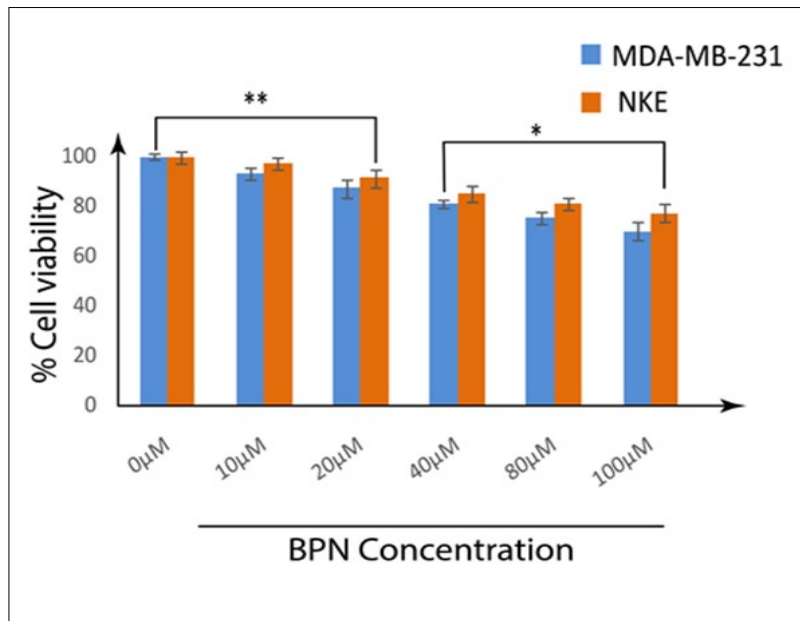
η = Refractive index of solvent. Here Φ measurements were performed using Rhodamine B in ethanol as standard [$\Phi = 0.49$]

The fluorescence quantum yield of **BPN** and **BPN-N₂H₄** product was calculated by taking Rhodamine B ($\Phi = 0.49$ in ethanol) as standard.

$\eta_s = 1.3614$ (for ethanol); $\eta_x = 1.479$ (for DMSO)

The quantum yield of **BPN** was calculated using the above equation and the value is 0.0075.

The quantum yield of **BPN-N₂H₄** adduct was calculated using the above equation and the value is 0.6193.



FigureS21: Cell survivability of MDA-MB 231 and NKE cells exposed to different probe **BPN** concentration. Data are representative of at least three independent experiments and bar graph shows mean \pm SEM, ** $p < 0.001$, * $p < 0.01$ were interpreted as statistically significant, as compared with the control.

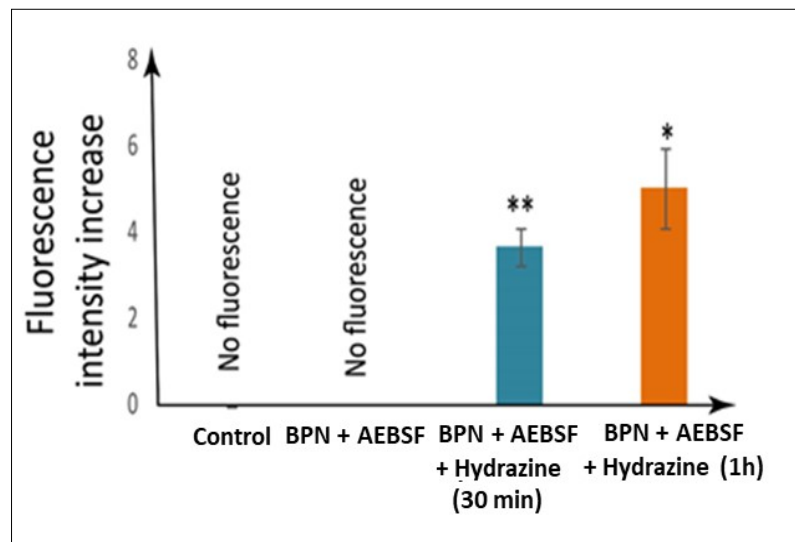


Figure S22: Pictorial fluorescence intensity variation of untreated MDA-MB 231 cells (Control), cells treated with probe **BPN** (10µM) + AEBSF(1 mM), probe **BPN** (10µM) + AEBSF (1 mM) + Hydrazine together after 30 min and 1h, incubation period.

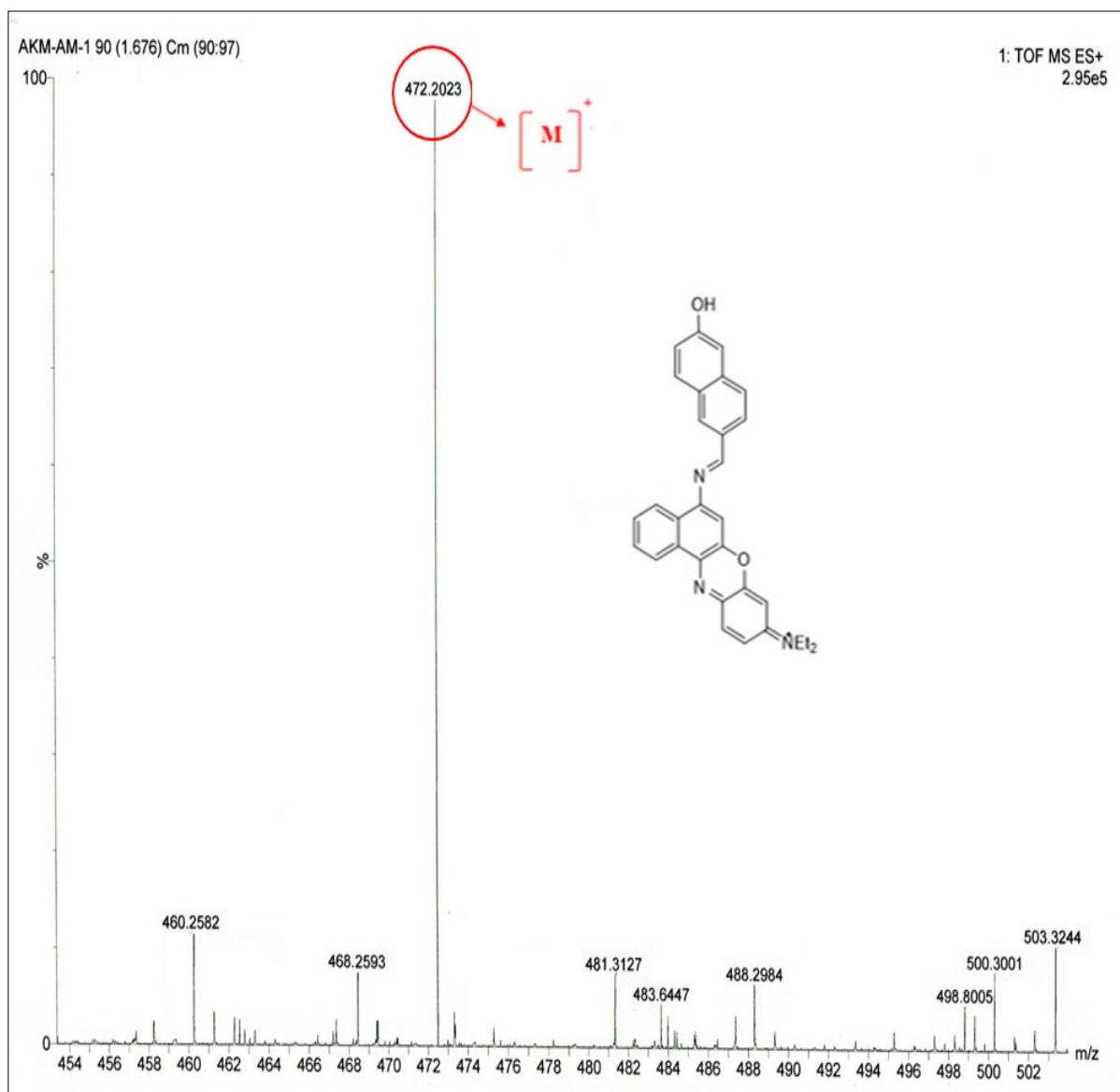


Figure S23: HRMS of BPN-N₂H₄ adduct.

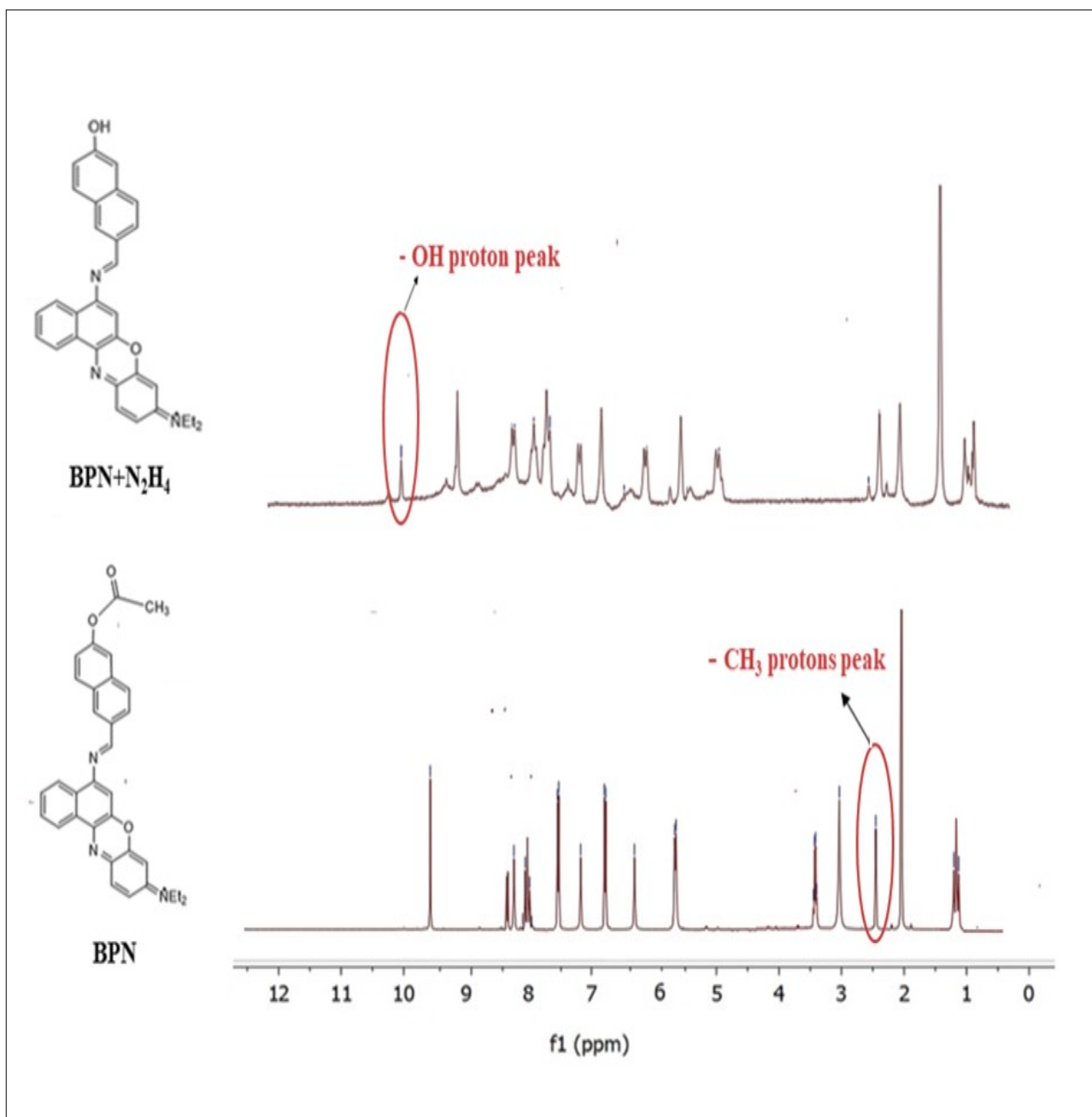
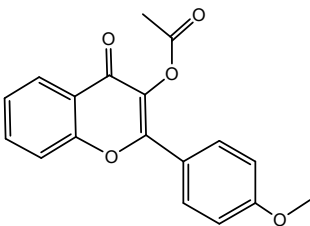
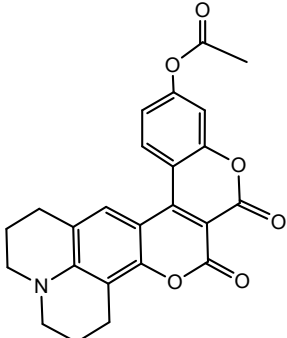
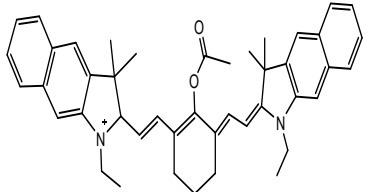
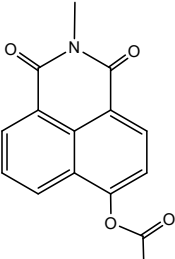
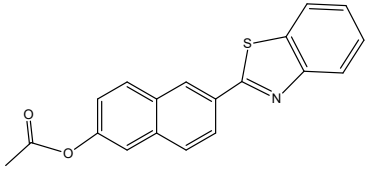
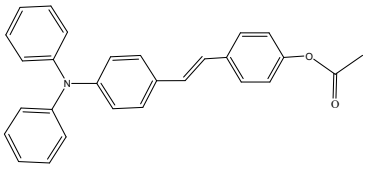
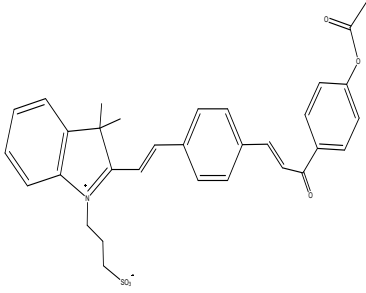
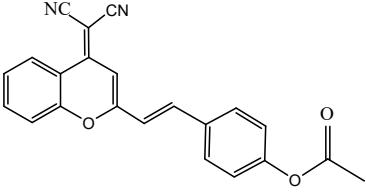
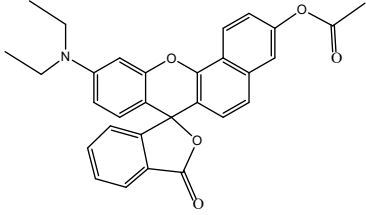
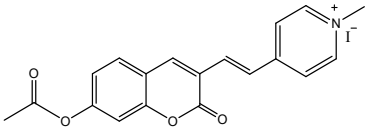
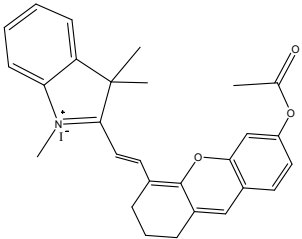
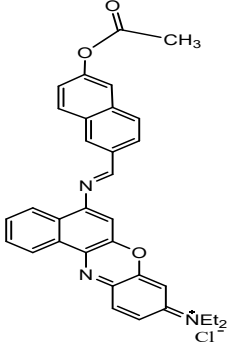


Figure S24: ¹H NMR titration of probe **BPN** with hydrazine.

Table S2: Comparison data of previously reported N₂H₄ sensors with current data

Sl. No	Probe structure	Excitation	Emission in presence of hydrazine	Detection limit	Response time	Application	Reference
1.		370 nm	415 nm [Ⓜ] (N* form) and 540 nm [Ⓜ] (T* form)	10 μM	60 min	Live stem cell and <i>invivo</i> zebrafish imaging	[1]
2.		480 nm	542 nm [Ⓜ]	5.4 ppb	10 min	Live HeLa cell and <i>invivo</i> zebrafish imaging	[2]
3.		540 nm [Ⓜ] and 730 nm [Ⓜ]	662 nm [Ⓜ] to 825 nm [Ⓜ]	2.56 ppb	7 min	Live cell, kidney tissue and <i>invivo</i> mouse body imaging	[3]
4.		385 nm	445 nm [Ⓜ] to 545 nm [Ⓜ]	9.40 nM	5 min	Live cell and <i>invivo</i> zebrafish imaging	[4]

5.		-	390 nm ² to 508 nm ²	0.96 μM	60 min	Live HeLa cell imaging	[5]
6.		350 nm	440 nm ²	8.47 nM	180s	Live cancer cell imaging	[6]
7.		430 nm	532 nm ²	1.72 ppb	-	Livecell, kidney tissue and <i>invivomous</i> e body imaging	[7]
8.		560 nm	680 nm ²	57 nM	1 min	(a)Detection in living cells (MCF- 7 cells); (b) Detection of hydrazine in solution by test kits.	[8]
9.		592 nm	654 nm ²	3.4 ppb	-	Live HeLa cell imaging.	[9]

10.		510 nm	559 nm ²	-	60 min	Live cell imaging	[10]
11.		675 nm	706 nm ²	5.4 ppb	10 min	Livecell, kidney and <i>invivo</i> mouse body imaging	[11]
12.		590 nm	725 nm ²	4.5 × 10 ⁻¹⁰ M	4s	Livecell imaging and vapor phase detection by test strips.	Our Work

References:

- [1] B. Liu, Q. Liu, M. Shah, J. Wang, G. Zhang and Y. Pang, *Sens. Actuators, B*, 2014, **202**,194–200.
- [2] Q. Fang, L. Yang, H. Xiong, S. Han, Y. Zhang, J. Wang, W. Chen and X. Song, *Chinese Chem. Lett.*, 2019, 2–5.
- [3] Y. Song, G. Chen, X. Han, J. You and F. Yu, *Sens. Actuators, B*, 2019, **286**, 69–76.
- [4] X. Xia, F. Zeng, P. Zhang, J. Lyu, Y. Huang and S. Wu, *Sens. Actuators, B*, 2016, **227**, 411-418.
- [5] C. Liu, K. Liu, M. Tian and W. Lin, *Spectrochim. Acta A*, 2019, **212**, 42–47.
- [6] X. Wang, G. Ding, Y. Wang, S. Mao, K. Wang, Z. Ge, Y. Zhang, X. Li and C. H. Hung, *Tetrahedron Lett.*, 2020, **76**, 131726.
- [7] T. Li, J. Liu, L. Song, Z. Li, Q. Qi and W. Huang, *J. Mater. Chem. B*, **2019**, 7, 3197–3200.
- [8] S. Zhang, D. Chen, L. Yan, Y. Xie, X. Mu, J. Zhu, *Microchem.*, **2020**, 157, 105066.

- [9] S. H. Guo, T. H. Leng, K. Wang, Y. J. Shen and C.Y. Wang, *Spectrochim. Acta A*, 2019, **223**, 117344.
- [10] Y.-Z. Ran, H.-R. Xu, K. Li, K. -K. Yu, J. Yang and X. -Q. Yu, *RSC Adv.*, **2016**, 6, 111016-111019.
- [11] J. Zhang, L. Ning, J. Liu, J. Wang, B. Yu, X. Liu, X. Yao, Z. Zhang and H. Zhang, *Anal. Chem.*, 2015, 87, 9101–9107.